

The Synergistic Anion-Binding Sites of Human Transferrin: Chemical and Physiological Effects of Site-Directed Mutagenesis[†]

Olga Zak, Katsuya Ikuta,[‡] and Philip Aisen*

Department of Physiology and Biophysics, Albert Einstein College of Medicine, 1300 Morris Park Avenue, Bronx, New York 10461

Received December 10, 2001; Revised Manuscript Received January 28, 2002

ABSTRACT: A defining feature of all transferrins is the absolute dependence of iron binding on the concomitant binding of a synergistic anion, normally but not necessarily carbonate. Acting as a bridging ligand between iron and protein, it completes the coordination requirements of iron to lock the essential metal in its binding site. To investigate the role of the synergistic anion in the iron-binding and iron-donating properties of human transferrin, a bilobal protein with an iron binding site in each lobe, we have selectively mutated the anion-binding threonine and arginine ligands that form an essential part of the electrostatic and hydrogen-bonding network holding the synergistic anion to the protein. Preservation of either ligand is sufficient to maintain anion binding, and therefore iron binding, in the mutated lobe. Arginine is a stronger ligand than threonine, and its loss weakens carbonate and therefore iron binding, but maintains the ability of nitrilotriacetate to serve as a carbonate surrogate. Replacement of both ligands abolishes anion binding and consequently iron binding in the affected lobe. Loss of anion binding in either lobe results in a monoferric protein binding iron in normal fashion only in the opposite lobe. Both monoferric proteins are capable of transferrin receptor-dependent binding and iron donation to K562 cells, but with diminished receptor occupancy by the protein bearing iron only in the N-lobe.

Transferrins comprise a class of iron-binding molecules functioning in the transport of iron in the circulation and delivery of iron for cellular needs. Vertebrate transferrins are bilobal molecules, products of a gene duplication and fusion events (1) that likely occurred more than 500 million years ago, with about 45% sequence identity in the two lobes and virtually identical iron-binding sites, one in each lobe. A traditional classification of vertebrate transferrins distinguishes three types: serum transferrin, or serotransferrin; ovotransferrin or egg white transferrin (formerly known as conalbumin); and lactoferrin, originally isolated from milk but also found in a wide variety of extracellular fluids and secretions. All of these bear nearly identical iron-binding sites but otherwise differ in their chemical and physiological properties. The human transferrin molecule experiences more than 100 cycles of iron binding and release during its 10-day lifetime in the circulation(2), so that understanding the mechanisms of iron binding and release is crucial to understanding the biological activities of transferrin.

A defining feature of all transferrins is the absolute dependence of iron binding on concomitant binding of a synergistic anion, normally but not necessarily carbonate. Other anions may fulfill the anion requirement when (bi)-carbonate is absent in solution; NTA¹ is one example of a

replacement for carbonate. In vertebrate transferrins, carbonate acts as a bidentate ligand for iron and is anchored to the protein by a network of hydrogen bonds, most importantly with the terminal NH₂ groups of an arginine residue, the OH group of a threonine, and the peptide nitrogen of a helix protruding into the binding cleft of each lobe (3). Binding of NTA does not involve the arginine, but the structure of NTA permits stabilizing interactions with peptide nitrogens of a serine-alanine-glycine sequence in the N-lobe of hen ovotransferrin (4), corresponding to residues 125–127 of the human N-lobe and residues 457–459 of the human C-lobe where threonine replaces serine.

The initial step in the interaction of iron-bearing transferrin with most iron-requiring cells is the binding of the protein to specific transferrin receptors. The complex of transferrin and receptor is then internalized to an endosome in which lowering of pH, among other still poorly understood factors, induces release of iron for export to the cytoplasm via the iron-transporter DMT1 (5). A critical step during the iron-donating interaction of transferrin with cells appears to be protonation and freeing of the synergistic anion, thereby disrupting the iron–protein complex (6). In an *in vitro* model of iron release to cells, lowering of pH in the presence of

[†] This work was supported in part by Grants 5 RO1 DK15056 and 1 PO1 DK55495 from the National Institutes of Health, U.S. Public Health Service.

* To whom correspondence should be addressed.

[‡] Permanent address: Third Department of Internal Medicine, Asahikawa Medical College, 2-1 Midorigaoka-Higashi, Asahikawa 078-8510, Japan.

¹ Abbreviations: NTA, nitrilotriacetate; SDS–PAGE, sodium dodecylsulfate polyacrylamide gel electrophoresis; EPR, electron paramagnetic resonance; cpm, counts per minute; Con A, concanavalin A.; BHK, baby hamster kidney; Tf, full-length human transferrin; FBS, fetal bovine serum; mT, milliTesla; rTf, recombinant full-length transferrin; TfR, transferrin receptor; PPi, pyrophosphate; Tf-Fec, monoferric native transferrin loaded in the C-lobe; rNlobe, recombinant N-lobe (residues 1–337) of transferrin.

iron chelators leads to discharge of iron from the protein because of freeing of the synergistic carbonate (7).

Understanding the binding of the synergistic anion is therefore central to understanding iron release from transferrin in cells and in vitro. To investigate further the relative contributions of the anion-binding ligands to the strength of iron-binding and to the specificity of the ligands for the physiological carbonate anion and its NTA surrogate, we have made a series of mutations in the carbonate-binding threonine and arginine residues of the N-terminal and C-terminal lobes of full-length transferrin and in the N-lobe by itself (residues 1–337). Spectroscopic, kinetic, anion-binding, and physiological properties of the mutants were substantially altered, providing further insights into the synergistic anion-binding functions of transferrins.

MATERIALS AND METHODS

Reagents and Proteins. Standard laboratory reagents, of the highest quality available, were obtained from Sigma-Aldrich and Fisher Scientific. Millipore-Q water was used for all experiments and preparations. Lyophilized iron-saturated human transferrin was purchased from Boehringer-Mannheim and stored at -20°C . The protein gave a single band on SDS–PAGE electrophoresis under reducing conditions and exhibited the expected absorbances at 280 and 465 nm. Native and recombinant transferrins were freed of iron and reloaded by established methods (8). A polyclonal antibody to bovine transferrin (Calbiochem) was raised in hens and used for western blotting as purified IgY (Washington Biotechnology).

Spectroscopic Studies. Optical spectra were recorded on an Aviv-Cary Model 14-DS spectrophotometer. A Bruker 200D X-band EPR spectrometer with ESP 300 upgrade and Gunn diode microwave source was used for obtaining EPR spectra. Standard conditions were as follows: microwave power, 10 mW; microwave frequency, 9.514 GHz; modulation amplitude, 1 mT. Sample temperatures were set at 100 K using a Bruker ER 4111 variable temperature apparatus. Receiver gains varied with sample concentrations but were generally near 2.5×10^5 . Except as noted, spectra were recorded with samples in 0.05 M HEPES, 100 mM NaCl, and pH 7.4.

Iron Release Kinetics. Rates of iron release from transferrins were measured at 25°C by a spectrofluorometric method (9) using a Photon Technology International Model QM-200-4SE instrument. Entrance slits were set to 2 nm and exit slits to 4 nm.

Electrophoresis Studies. SDS–PAGE studies for establishing the purity of recombinants were performed under reducing conditions with a Pharmacia PhastSystem using 12.5% homogeneous polyacrylamide gels.

Radiolabeling. Proteins were labeled with ^{125}I by the BioRad Enzymobead method or by the iodine monochloride procedure (10). After chromatography on BioRad PD10 columns, more than 95% of the radioactivity in labeled proteins was precipitable in 20% trichloroacetic acid/4% phosphotungstic acid. Labeling with ^{59}Fe used ^{59}Fe –NTA in 1:2 proportion. Gamma counting was carried out in a TM Analytic GammaTrac 1193 counter to a statistical accuracy better than $\pm 3.2\%$ (1000 cpm above background).

Mutagenesis, Expression, and Purification of Recombinant Transferrins. Mutagenesis in the pNUT vector bearing non-

glycosylated full-length or N-lobe transferrin coding sequences, gifts from Drs. Anne Mason and Ross MacGillivray, was carried out using the Stratagene QuikChange kit. Mutagenic primers were as follows:

T120A	GTCCTGCCACGCGGGTCTAG
R124S	GGTCTAGGCAGTTCCGCTGGGTGG
T452A	GTCCTGCCATGCTGCAGTTGG
R456S	GCAGTTGGCAGTACCGCTGG

and their complements. Double mutations were produced sequentially using appropriate pairs of the above primers. Changed bases are underlined; mutations were verified by sequencing of the entire coding sequence for the isolated N-lobe or the full-length protein.

Expression of recombinant transferrins was accomplished with BHK 21 cells in DMEM-F12 medium containing 0.5–1% Ultoser G (11, 12). All media were enriched with 10 μM $\text{Fe}(\text{NTA})_2$ before isolation and purification of recombinant proteins. Isolation of the secreted recombinant proteins was carried out by anion exchange chromatography using an Amersham-Pharmacia Äkta Explorer 10 system and Poros 50HQ media (PerSeptive Biosystems) with elution by a gradient of 0–200 mM NaCl in 20 mM Tris, pH 7.0. Final purification was achieved with ConA chromatography to separate residual glycosylated bovine transferrin from recombinant nonglycosylated full-length transferrin. Size-exclusion chromatography on a Pharmacia Hi-Load 16/60 Superdex 75 column separated recombinant N-lobes from other proteins in the culture media. Final proteins exhibited expected mobilities and were homogeneous by SDS–PAGE electrophoresis and free of bovine transferrin by western blotting with a polyclonal anti-bovine transferrin chicken antibody.

Cell Studies. K562 cells were grown in RPMI 1640 medium containing 10% FBS and harvested when cell densities were near $10^7/\text{ml}$. To free them of adventitious transferrin, we incubated cells twice for 15 m at 37°C in RPMI 1640 without serum and washed them each time. Transferrin binding and iron uptake studies followed methods previously described (12). In each experiment, comparative studies of each mutant protein and native transferrin as control were carried out with the same harvesting of cells, but different harvestings were used for different experiments. Receptor occupancies and receptor-protein binding energies were calculated from the expressions

$$\text{receptor occupancy} = \frac{K_a[\text{protein}]}{1 + K_a[\text{protein}]} \quad (1)$$

and

$$\text{binding energy} = -RT \ln K_a \quad (2)$$

where K_a is the association constant for binding of transferrin to receptor, R is the gas constant, and T is the absolute temperature.

RESULTS

Visible Spectroscopy. All of the anion-binding site mutants showed the salmon-pink color of native transferrin, with absorption peaks in the range 465–472 nm (Table 1). Its

Table 1: Visible Absorbance Maxima of Transferrin Mutants

mutant	absorbance maximum (nm)	A_{465}/A_{280}
rNlobe(T120A)	465	0.043
rNlobe(R124S)–NTA ^a	467	
rTf(R456S)–CO ₃ ^a	465	0.041
rTf(R456S)–NTA ^a	472	
rTf(T120A–R124S)	465	0.027
rTf(T452A–R456S)	465	0.024

^a Synergistic anion.

ratio of absorbances at 465 to 280 nm provides a good indication of the iron occupancy of a transferrin. The ratio expected of diferric transferrin is near 0.042, that of apotransferrin near zero, and that of monoferric transferrin intermediate between the two (14). $A_{465}:A_{280}$ ratios of 0.041 and 0.043 were found in rTf(R456S) and rNlobe(T120A), respectively, both comparable to that given by native diferric transferrin and therefore indicating that little disruption of protein tyrosinate ligands to iron had occurred as a result of the mutations. Mutations of threonine and arginine ligands in a lobe result in monoferric proteins incapable of binding iron in the mutated lobe, as indicated by their absorbance ratios. The double mutants, then, can provide tools for studying the chemical and physiological properties of a lobe in full-length transferrin without complexities introduced by scrambling of iron between lobes.

EPR Spectroscopy of N-Lobe Mutants. Presentation of one $\text{Fe}^{3+}(\text{NTA})_2$ per molecule of rNlobe(R124S) yields a preparation with an EPR spectrum showing only the features expected when NTA occupies the synergistic anion site (Figure 1A). The NTA-type spectrum persists unchanged despite incubation in 10 mM bicarbonate for 96 h. When loaded with iron as Fe^{2+} and allowed to autoxidize in the presence of 10 mM bicarbonate, the resulting spectrum shows the $g' = 4.3$ splitting characteristic of the carbonate complex (Figure 1B), although the spectrum is not quite identical to that of wild-type N-lobe with carbonate as synergistic anion. Mutation of the threonine anion-binding ligand, T120A, while preserving the arginine ligand and loading with $\text{Fe}(\text{NTA})_2$ in the presence of ambient bicarbonate, leads to a complex with a splitting in its Fe^{3+} EPR spectrum that suggests occupancy of the anion-binding site by carbonate (Figure 1C). EPR spectroscopy therefore indicates that either the arginine or threonine ligand is sufficient for carbonate to serve as the synergistic anion. Since loss of arginine disables replacement of NTA by carbonate, arginine appears as the stronger ligand for the physiological anion.

The EPR spectrum of the T120A–R124S mutant (not shown), which carries iron only in the C-lobe, is nearly identical to that of the proteolytically derived C-lobe (13), exhibiting a splitting of 3.7 mT in the $g' = 4.3$ signal compared to the splitting of 3.9 mT in the isolated C-lobe and 2.7 mT in the recombinant N-lobe. EPR spectroscopy verifies that the double mutation destroys synergistic anion binding and therefore iron binding but leaves iron binding intact in the unaltered lobe.

EPR Spectroscopy of C-Lobe Mutants. EPR spectra of the arginine mutant in full-length transferrin, rTf-R456S, are shown in Figure 2. When the apoprotein is loaded with $\text{Fe}^{3+}(\text{NTA})_2$ under nitrogen (to exclude CO_2 and hence bicarbonate), the EPR spectrum is characteristic of that obtained when

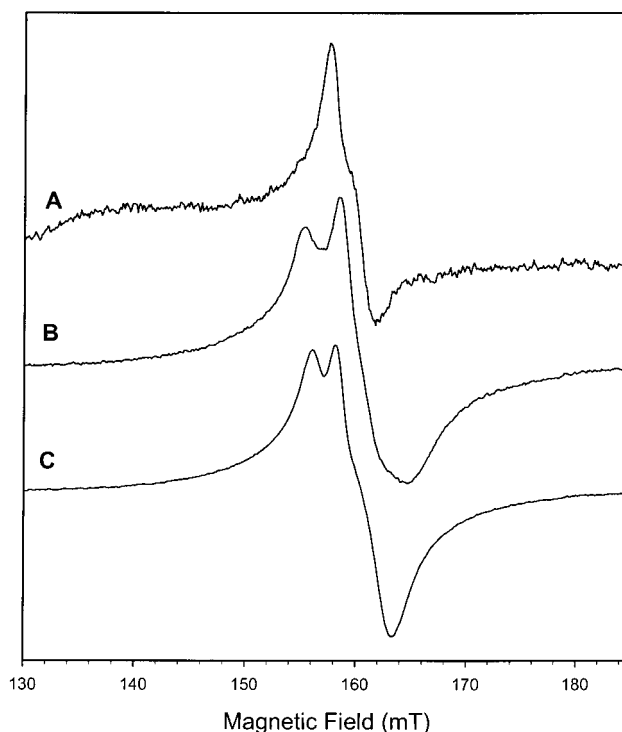


FIGURE 1: EPR spectra of N-lobe mutants. A, rNlobe(R124S) loaded with $\text{Fe}^{3+}(\text{NTA})_2$. The spectrum is not changed by the addition of 0.1 mM bicarbonate; B, rNlobe(R124S) loaded with Fe^{2+} in the presence of 0.1 M bicarbonate and allowed to stand 96 h in air; C, rNlobe(T120A) loaded with $\text{Fe}^{3+}(\text{NTA})_2$ in 20 mM Tris, pH 8.0, with ambient bicarbonate.

NTA serves as the synergistic anion (Figure 2A) (15). Addition of 10 mM bicarbonate to the sample results after 3 h in a spectrum that is a composite of the NTA and carbonate spectra (Figure 2B); the relative intensity of the carbonate component increases over the next 2 days (Figure 2C), remaining constant thereafter while the NTA component persists. The indication, then, is that carbonate, which easily and quickly displaces NTA from both specific sites of native transferrin (15), is unable to compete with NTA for the synergistic binding site of the mutated C-lobe in rTf(R456S). When iron is added to the mutant protein as Fe^{2+} and allowed to autoxidize, the resulting spectrum (Figure 2D) approximates that of monoferric native transferrin loaded in the C-lobe (Figure 2E) with a characteristic splitting of the $g' = 4.3$ line, suggesting the presence of carbonate as the synergistic anion in both sites of the mutant protein in the absence of competing NTA. EPR spectra of Figure 2E and diferric native transferrin are virtually identical except for the difference in splitting of the $g' = 4.3$ signal, too small to be apparent in the Figure. The R \rightarrow S mutation therefore exerts comparable effects in both lobes.

A splitting of 2.8 mT is present in the $g' = 4.3$ EPR line of the rTf(T452A–R456S) C-lobe mutant of full-length transferrin (not shown), as expected of iron occupancy in the N-lobe alone. In the C-lobe as well as the N-lobe, the double mutation abolishes iron binding without disturbing iron binding in the unchanged lobe.

Kinetics of Iron Release from N-Lobe Mutants. Rates of iron release to pyrophosphate from wild-type and mutant N-lobe mutants were measured at pH 7.4 (Table 2); pyrophosphate (or another iron acceptor) is required for release to occur. In all cases release is measurably slower in

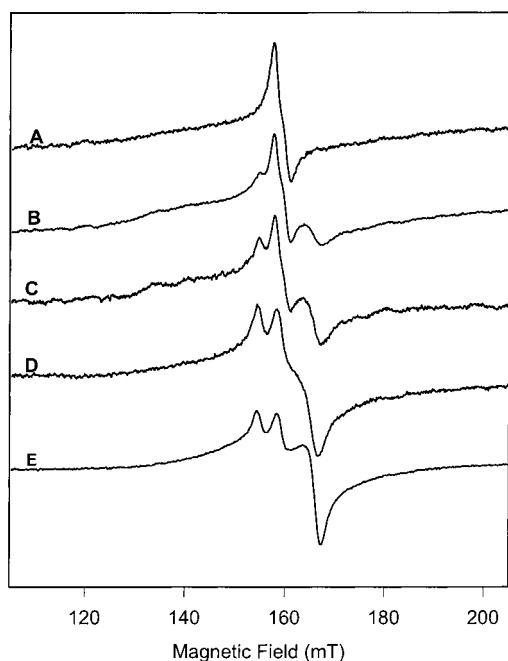


FIGURE 2: EPR spectra of rTf(R456S). A, immediately after the addition of 2 Fe^{3+} /Tf under nitrogen; B, 3 h after the addition of 0.1 mM bicarbonate to sample A; C, 70 h after the addition of 0.1 mM bicarbonate to sample A; D, rTf(R456S) loaded with 2 Fe^{2+} in the presence of 0.1 mM bicarbonate and allowed to stand 19 h in air; E, native monoferric Tf loaded in the C-lobe (for comparison). Protein concentrations varied from sample to sample, so all spectra normalized to provide similar peak-to-peak amplitudes. A low-field step-function artifact has been excluded from spectrum E.

Table 2: Kinetics of Iron Release from Recombinant N-Lobes^a

protein	[PPi] (mM)	[Cl ⁻] (mM)	k_{obs} ($\text{s}^{-1} \times 10^4$) ^b
rTf(T452A–R456S) ^c	100	100	9.1
	100	600	8.7
rNlobe, wild type	100	100	7.4
	100	600	7.0
rNlobe(T120A)	20	100	7.5
	20	600	3.0
rNlobe(R124S)	1	100	27
	1	600	21

^a All proteins with carbonate as the synergistic anion. ^b Measured in duplicate, with variations $< \pm 5\%$ of mean. ^c Full-length monoferric transferrin loaded in the N-lobe.

600 mM NaCl than in 100 mM NaCl, in accord with previous studies showing a retarding effect of ionic strength on release kinetics in the N-lobe (16, 17), in contrast to the accelerating effect observed in the C-lobe (9, 18). The negative effect is consistent with competition between chloride and pyrophosphate for a binding site in the N-lobe sufficiently close to the metal-binding site for ligand exchange from protein to iron acceptor to occur. Since the effect is preserved in the synergistic anion ligand mutations, this putative binding site must be distinct from the synergistic anion site.

Release is slightly faster from the N-lobe of full-length transferrin than from the isolated N-lobe, again showing interlobe interactions (19, 20) even if the C-lobe is unable to accept iron.

A striking difference is present in release rates from the threonine and arginine mutants, with the latter much more facile in giving up its iron. To achieve rates comparable to

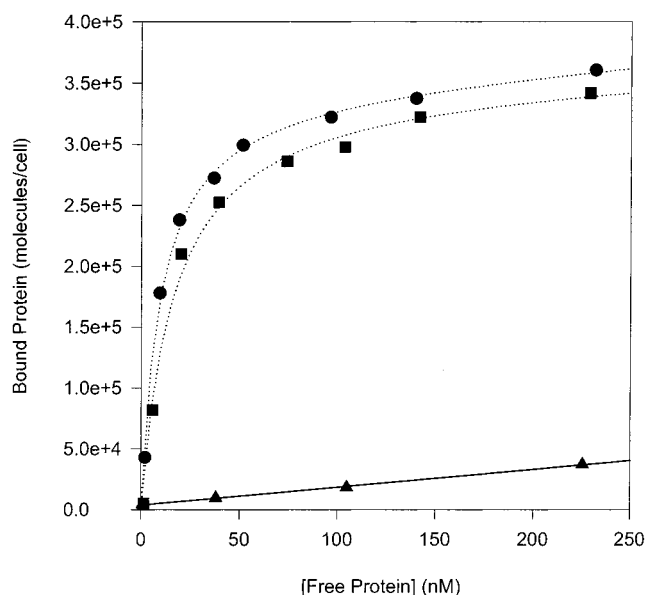


FIGURE 3: Binding of native diferric Tf and diferric rTf(R456S) to K562 cells at 4 °C. ●, native diferric Tf; ■, diferric rTf(R456S); ▲, diferric rTf(R456S) in the presence of 100-fold molar excess of unlabeled diferric Tf; ·····, fitted binding isotherms after correction for nonspecific binding; —, regression line.

those obtained with wild-type N-lobes, the pyrophosphate concentration must be reduced from 100 to 20 mM for rNlobe (T120A), but release is three times faster from rNlobe(R124S) to 1 mM pyrophosphate than from the wild-type lobe N-lobe to 100 mM pyrophosphate. Since iron release and anion lability are linked, the arginine ligand again appears as the principal anchor for the synergistic anion.

Binding of C-Lobe Mutants and Uptake of Their Iron by K562 Cells. A comparison of the binding of diferric Tf and diferric rTf(R456S) by K562 cells at 4 °C is shown in Figure 3. The curve-fitted binding constant for the mutant, $6.0 \times 10^7 \text{ M}^{-1}$, is about 60% of that found for the native protein, $1.0 \times 10^8 \text{ M}^{-1}$, so that the binding energy for the mutant is $>95\%$ of the binding energy for the native protein. Each protein is recognized by the same number of binding sites, 350 000, verifying that receptor interactions of the two proteins are similar. Rates of iron uptake at 37 °C from the proteins under identical conditions are similar: 230 000 atoms/cell/m for diferric Tf and 210 000 atoms/cell/m, measured at 90 m (Figure 4). At the concentration of proteins used, $2.7 \times 10^{-7} \text{ M}$, receptors would be at least 94% saturated by either protein so that the rates of iron uptake normalized to receptor occupancy are also similar for the two proteins.

Mutation of both anion-binding ligands of the C-lobe yields a protein, rTf(T452A–R456S), incapable of holding iron in that lobe but able to accept iron in the unchanged N-lobe. Binding of the resulting monoferric protein loaded in the N-lobe to K562 cells at 4 °C is shown in Figure 5. The binding isotherm indicates saturable binding inhibitable by native diferric Tf and is therefore presumed to be specific for transferrin receptors. We have found that the isolated C-lobe, free of N-lobe sequences, is capable of specifically binding to transferrin receptors (21, 22), and there is general agreement that the isolated N-lobe cannot complex with the receptor. It appears likely, therefore, that the mutated iron-free C-lobe of full-length transferrin with the iron-occupied

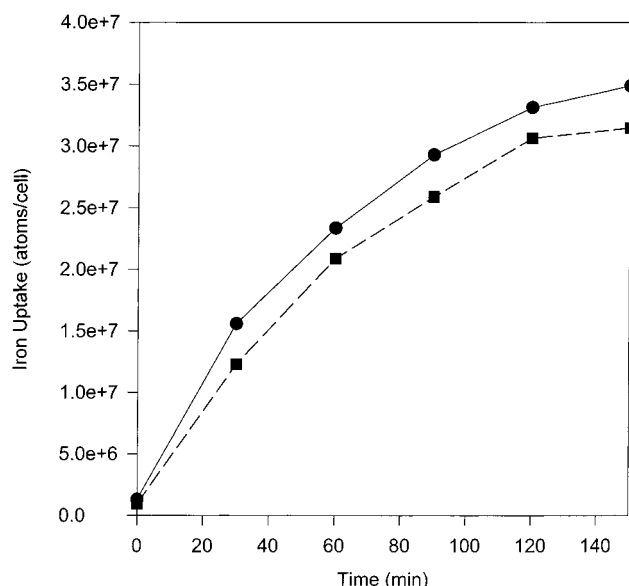


FIGURE 4: Iron uptake by K562 cells from native diferric Tf and diferric rTf(R456S) at 37 °C and identical concentrations of proteins (2.5×10^{-7} M). Rates of uptake are within 10% of each other throughout the course of the experiment. ●, native diferric Tf; ■, diferric rTf(R456S).

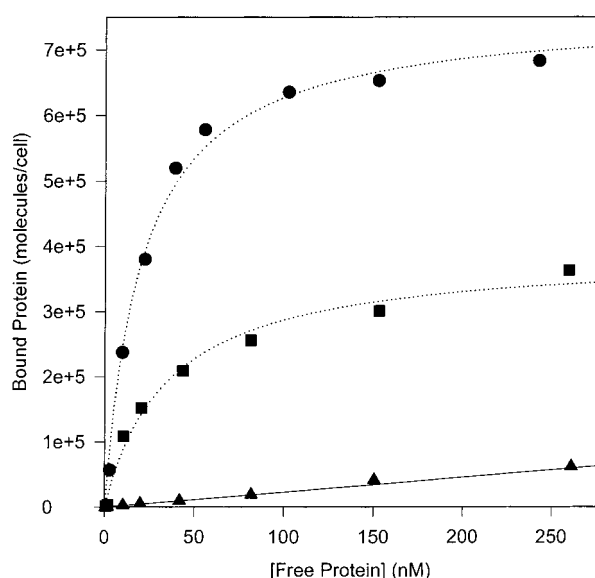


FIGURE 5: Binding by K562 cells at 4 °C of native diferric Tf and full-length monoferric rTf(T452A-R456S) bearing iron in the N-lobe. The double mutation abolishes anion binding, and therefore iron binding, in the C-lobe of transferrin. Nevertheless, the mutant loaded in the unchanged N-lobe binds to K562 cells in saturable manner inhibitable by 100-fold molar excess of unlabeled diferric Tf, consistent with retention of receptor-binding conformation in the altered C-lobe. ●, native diferric Tf; ■, rTf(T452A-R456S); ▲, rTf(T452A-R456S) in the presence of 100-fold molar excess of unlabeled diferric Tf; ····, fitted binding isotherms after correction for nonspecific binding; —, regression line.

wild-type N-lobe retains the receptor-recognition conformation. The binding constant for the monoferric mutant, $2.8 \times 10^7 \text{ M}^{-1}$, is about 60% of that of the native diferric protein, $4.9 \times 10^7 \text{ M}^{-1}$, so that the binding energies are also comparable (−40 and −41 kJ, respectively), but only about half as many sites are occupied by the mutant, 390 000, as by the native protein, 760 000. The rate of iron uptake from the mutant, 93 000 atoms/cell/m (calculated after 150 m of

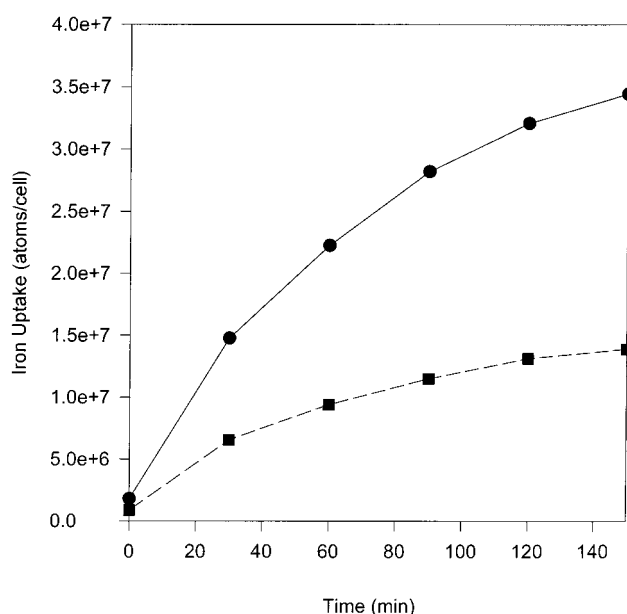


FIGURE 6: Iron uptake by K562 cells at 37 °C from native diferric Tf and full-length monoferric rTf(T452A-R456S), bearing iron only in the N-lobe, at identical concentrations of proteins (2.5×10^{-7} M). ●, native diferric Tf; ■, rTf(T452A-R456S). The rate of uptake from the double mutant is about 40% of that from the native protein throughout the course of the experiment.

incubation), is about 40% of that from diferric transferrin, 230 000 atoms/cell/m (Figure 6), consistent with the mutant's reduced binding to cells and its inability to accept iron in the C-lobe. In these experiments, receptor saturation is calculated as 87% for the mutant and 91% for the native protein so that a difference in receptor occupancy does not account for the difference in iron uptake.

Binding of Mutant rTf(T120A-R124S) and Uptake of Its Iron by K562 Cells. In contrast, the N-lobe mutant of full-length transferrin, rTf(T120A-R124S), bears iron only in its C-lobe, displaying an EPR spectrum (not shown) with a 3.7 mT splitting of the $g' = 4.3$ signal characteristic of the C-lobe (14). The mutant is recognized by nearly the same number of sites as native diferric transferrin, 288 000 for the former and 295 000 for the latter (Figure 7), in keeping with a primary receptor-recognition function of the iron-occupied C-lobe (21). The apparent binding constant for the mutant, $2.1 \times 10^7 \text{ M}^{-1}$, however, is only about 30% of that of the native protein, $7.1 \times 10^7 \text{ M}^{-1}$, consistent with the contribution of the iron-loaded N-lobe to the strength of receptor binding (21, 22). The rate of iron uptake from transferrin with the doubly mutated N-lobe is about 55% of the rate from native transferrin, as expected from a monoferric compared to a diferric protein (Figure 8). The concentration of proteins, 380 nM, is sufficient for 90% saturation of receptors by the mutant, and >95% saturation by the native protein, so that a difference in receptor occupancy is not likely to be a significant factor in the difference in rates of iron uptake.

DISCUSSION

A feature of all vertebrate transferrins, and the bacterial transferrins of *Neisseria* and *Hemophilus* (23), is the interdependence of iron binding and anion binding: neither metal nor anion is tightly bound at either specific site of the

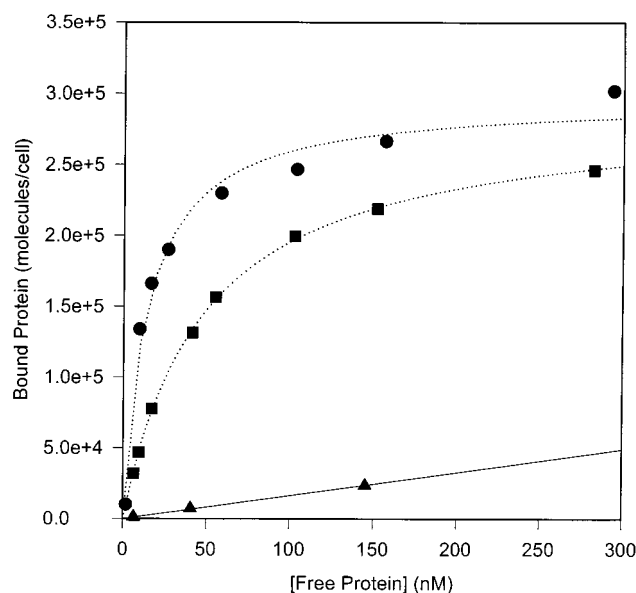


FIGURE 7: Binding by K562 cells at 4 °C of native diferric Tf and full-length monoferric rTf(T120A-R124S), bearing iron only in the C-lobe. The double mutation abolishes anion binding, and therefore iron binding, in the N-lobe of transferrin. The mutant loaded in the unaltered C-lobe binds to K562 cells in saturable manner inhibitable by 100-fold molar excess of unlabeled diferric Tf and to nearly the same number of binding sites as that found in the native protein (288 000 and 295 000, respectively) consistent with retention of receptor-binding conformation, although the apparent binding affinity is only about 30% of that found in the native protein ($2.1 \times 10^7 \text{ M}^{-1}$ compared to $7.1 \times 10^7 \text{ M}^{-1}$). ●, native diferric Tf; ■, rTf(T120A-R124S); ▲, rTf(T120A-R124S) in the presence of 100-fold molar excess of unlabeled diferric Tf; ·····, fitted binding isotherms after correction for nonspecific binding; —, regression line.

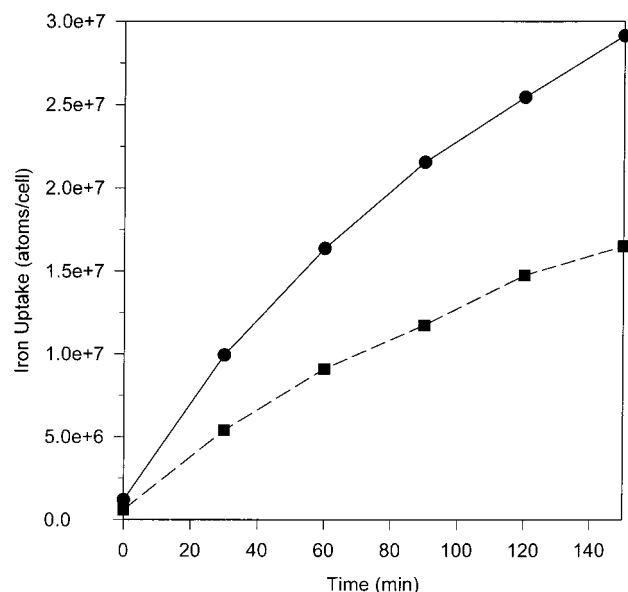


FIGURE 8: Iron uptake at 37 °C by K562 cells from native diferric Tf and full-length monoferric rTf(T120A-R124S) at identical concentrations of proteins ($2.5 \times 10^{-7} \text{ M}$). ●, diferric Tf; ■, rTf(T120A-R124S). The rate of uptake from the double mutant is about 55–60% of that from the native protein throughout the course of the experiment.

protein unless both are present. This dependence of metal binding on concomitant binding of a suitable anion has led to the designation of the anion as “synergistic” (24), a usage which has gained currency for the incisive insight it provides.

The crystal structure of human lactoferrin (25) first revealed the ligands of iron and its synergistic carbonate anion, and subsequent studies verified similarities with ovotransferrin (26) and human transferrin (27). The carbonate binds in bidentate fashion to the iron and is anchored to the protein by hydrogen bonding and electrostatic interactions predominantly involving Arg 124 in the N-lobe (456 in the C-lobe), Thr 120 (452) and the positively charged N-terminus of a helix (designated helix 5) protruding into the binding cleft, residues 124–137 (456–470). Because of its dual role in hydrogen and electrostatic bonding and its strong positive charge, the Arg ligand has been thought to provide the strongest link from anion to protein. In exploring the role of the anion-binding site in the iron-binding and iron-donating functions of transferrin, we have selectively mutagenized the Arg and Thr ligands of the N- and C-lobes of human transferrin, examining the effects of the mutations on the spectroscopic, kinetic, and iron-donating properties of the proteins.

Optical Absorbance Studies. When devoid of iron, transferrins are colorless, but when bearing iron, they display a characteristic salmon-pink color that has been ascribed to a tyrosine phenolate-to- Fe^{3+} charge-transfer transition near 465 nm (28). Loss of the Tyr95 ligand is accompanied by loss of about half the intensity of the 465 nm peak (29), suggesting that both tyrosine ligands participate in the charge transfer transition. The synergistic anion has no direct role in the visible absorbance, as changes in the anion produce relatively little effects on the absorption band (15, 24). Mutations of a single anion-binding residue, either arginine or threonine, and whether in N- or C-lobes, preserve the iron-binding function of transferrin and its associated absorption peak in the range 464–472 nm (Table 1). The single mutations therefore do not perturb the tyrosinate coordination to Fe^{3+} .

EPR Spectroscopy of N-Lobe Mutants. The effects of the R \rightarrow S mutation on the EPR spectrum are best seen in the recombinant N-lobe where they are not merged with the unperturbed features of the C-lobe spectrum (Figure 1). Although the general features of the wild-type spectrum are present (similar to Figure 2E), the splitting of the $g' = 4.3$ signal is increased from 2.8 to 3.4 mT, indicating some distortion of the ligand geometry at the iron-binding site.

Mutating the hydrogen-bonding N-lobe threonine to an alanine, rNlobe(T120A), maintains carbonate binding (Figure 1C), and therefore iron binding, but with some minor changes in the EPR spectrum. Splitting of the $g' = 4.3$ signal is decreased from 2.8 to 2.0 mT, and the lines are distinctly narrowed. Nevertheless, the general features suggest that the ligand structure about the iron is little changed.

In contrast, mutation of the arginine and threonine anion ligands in the N-lobe destroys its anion-binding function, and therefore its iron-binding activity, again verifying the interdependence of anion- and iron-binding. Iron-binding in the C-lobe, as evidenced by a wild-type EPR spectrum, is unaffected by the double mutation in the N-lobe (not shown). The general conclusion is that either the arginine or threonine ligands is sufficient to maintain carbonate binding, but loss of both entails loss of anion binding and therefore of metal binding.

EPR Spectroscopy of C-Lobe Mutants. Mutation of Arg 456 to Ser does not affect the ability of the protein to accept

NTA as the synergistic ligand for binding iron (Figure 2A), consistent with crystallographic studies showing no interaction of NTA with the corresponding Arg in the iron-occupied N-lobe of ovotransferrin (4). Instead, the NTA is stabilized by hydrogen bonding to peptide nitrogens of Ser122, Ala123, and Gly124 of the ovotransferrin N-lobe (corresponding to residues 125–127 in human N-lobe) and the OH group of Thr117 (Thr 120). None of these should be affected by the R456S mutation. However, the binding of carbonate is substantially weakened so that the ability of the physiological anion to displace NTA, as in native transferrin (15), is lost (Figure 2B,C). When iron is presented as Fe^{2+} to full-length rTf(R456S) and allowed to autoxidize to Fe^{3+} in the presence of ambient CO_2 (Figure 2D), the anion-binding function can still be satisfied by carbonate. Thus, the threonine ligand of the anion and the positively charged N-terminus of helix 5 are sufficient to hold the physiological anion in place in each lobe.

Kinetics of Iron Release from Isolated N-Lobe. As indicated in earlier studies (16, 30), loss of the carbonate-binding arginine residue destabilizes iron binding in the N-lobes of human transferrin and lactoferrin, in accord with the present results (Table 2). To achieve comparable iron release rates from wild-type and mutant N-lobes to pyrophosphate at pH 7.4, we had to reduce the concentration of pyrophosphate from 100 to 1 mM. Loss of threonine 120, another participant in the hydrogen-bonding network that anchors carbonate to its protein host, also facilitates iron release, but much less strikingly than loss of arginine 124. Although either the arginine or threonine ligand by itself is sufficient for maintaining attachment of the synergistic carbonate, and therefore the iron, mutation of the arginine residue has the greatest effect on iron release. Arginine once again emerges as the more important ligand of synergistic carbonate.

Cell Studies. The predominant pathway of iron uptake from transferrin by iron-dependent cells is by high-affinity, saturable, receptor-mediated endocytosis (31); a receptor-independent, but low-affinity pathway has been described in cells of hepatic lineage (32). The mechanism of iron uptake via the former pathway is well understood: the complex of iron-bearing transferrin bound to cell-surface receptors is internalized to a proton-pumping endosome where the lowered pH and other factors promote iron release and reduction of iron from transferrin. The ferrous iron is then transported across the endosomal membrane by a specific transporter, DMT1 (33), for cellular needs or storage. The originally described TfR1 has recently been joined by a second receptor, TfR2 (34), but the relative importance of the two receptors in various cell types is not yet fully understood.

A variety of cell lines has been used in investigating transferrin binding and iron uptake. The K562 cell, of human hematopoietic origin, can be induced to express hemoglobin, and has often been taken as a model of the transferrin-dependent iron-requiring cell. It offers the advantage of a high receptor number, in the range of 350,000–1,000,000, relatively little nonspecific binding of transferrin, and exclusive or near-exclusive receptor-dependent uptake of transferrin iron. We have therefore chosen this cell for our studies of receptor binding and iron uptake.

Diferric rTf(R456S) binds in saturable fashion to the same number of sites on K562 cells as native diferric transferrin and with about 60% of the affinity of diferric Tf (Figure 3). The ability of the mutant protein to provide iron to the cells is close to that of the native protein (Figure 4). The indication, therefore, is that rTf(R456S) is recognized by transferrin receptors, TfR1 or TfR2 or both. This is not surprising, since mutation of the anion-binding arginine in the N-lobe of human lactoferrin leaves the overall conformation of the protein substantially unchanged (30) and so presumably preserves the binding conformation in the C-lobe of transferrin while leaving the N-lobe undisturbed.

Molecular mechanisms in the interaction of transferrin with transferrin receptors are still poorly understood. Transferrin experiences conformational changes upon binding and release of iron: binding of iron to a lobe is accompanied by a transformation from an open conformation to a closed state as the two domains of the lobe, enclosing the iron-binding cleft, rotate as rigid bodies about the hinging strands joining the domains (35, 36). Conformational changes associated with iron binding are thought to be critical to interactions of transferrin with transferrin receptors. Apotransferrin with both lobes in the open conformation is not recognized by cell-surface transferrin receptors at extracellular pH, 7.4 (37, 38), but is capable of binding to receptors at endosomal pH, 5.4 (39). Monoferric human transferrins are iron donors to human cells (although less effective than diferric transferrin) (12, 40). Both rabbit monoferric transferrins bind in specific fashion and donate iron to rabbit reticulocytes (41). In the last citation, however, the surprising finding is that rabbit apotransferrin also binds to rabbit cells, but with about 1/25th the affinity of diferric transferrin. Whether this discordance between rabbit and human transferrin-cell interactions is due to species or methodological differences is not clear.

Energy barriers between open and closed forms of the full-length apoproteins may be small (42) so that both forms are in equilibrium in solution, with packing forces determining the predominant crystal form. A conformation intermediate between open and closed states has been postulated (43) and perhaps observed in crystal structures of the N-lobe (27). Further indication of conformational flexibility in transferrin lobes is provided by the latter studies of N-lobe in two different crystal forms, orthorhombic and tetragonal, each of which is found in two conformers (27). In one of these (the “B” conformer of the orthorhombic form), the arginine moves sufficiently far away from the carbonate anion so that the distances between arginine amino nitrogens and carbonate oxygen exceed 4 Å, and both hydrogen bonds are therefore lost. Movement of the arginine in the corresponding conformer of the tetragonal form is less, and one hydrogen bond persists. A similar conformational flexibility may account for the finding that the C-lobe of crystallized apolactoferrin is closed in a crystal structure (35), but open in the solution structure (44) and in crystallized duck ovotransferrin (42).

Both monoferric transferrins created by double mutations at the synergistic anion site of a lobe are capable of binding to transferrin receptors and donating iron to K562 cells. Binding and release of iron to K562 cells by the N-lobe mutant, T120A–R124S loaded with iron in the C-lobe (Figures 7 and 8), are not unexpected since we have reported that the proteolytic or recombinant iron-bearing C-lobe of human transferrin, by itself, is necessary and sufficient for

receptor recognition and iron donation (21, 22). Receptor-binding and iron-donating activity by the T452A–R456S C-lobe mutant is somewhat surprising, however. The isolated N-lobe by itself, whether iron-free or iron-loaded, is incapable of binding to transferrin receptor in an iron-donating interaction with cells (21, 45), and neither full-length apotransferrin nor the iron-free isolated C-lobe is recognized by transferrin receptors (22, 37, 38). The presumption, therefore, is that the closed conformation of C-lobe is required for receptor recognition. The postulated ease of transitions between open and closed forms may explain the finding that full-length rTf(T452A–R456S) with an empty C-lobe but occupied N-lobe binds to K562 cells in a saturable manner inhibitable by native diferric transferrin and is therefore likely to involve specific transferrin receptors. Equilibrium between conformations capable of receptor-binding and conformations not recognized by receptor may then account for the diminished binding of this monoferric mutant to K562 cells. The iron-loaded N-lobe of the mutant, although incapable of binding by itself, may contribute to receptor binding of the C-lobe mutant by easing transition of the C-lobe between open and closed states as well as by direct interactions with receptor. Such an effect may also explain the near-normal binding to K562 cells of the C-lobe mutant, G394R, in which low-angle X-ray scattering reveals that lobe to be predominantly in the open conformation in solution (46). These remain speculations that must await structural analysis of the receptor-transferrin complex.

ACKNOWLEDGMENT

We are grateful to Ms. Jessica Muoio for her expert technical assistance in the purification of transferrin mutants.

REFERENCES

1. Park, I., Schaeffer, E., Sidoli, A., Baralle, F. E., Cohen, G. N., and Zakin, M. M. (1985) *Proc. Natl. Acad. Sci. U.S.A.* 82, 3149–3153.
2. Katz, J. H. (1961) *J. Clin. Invest.* 40, 2143–2152.
3. Shongwe, M. S., Smith, C. A., Ainscough, E. W., Baker, H. M., Brodie, A. M., and Baker, E. N. (1992) *Biochemistry* 31, 4451–4458.
4. Mizutani, K., Yamashita, H., Kurokawa, H., Mikami, B., and Hirose, M. (1999) *J. Biol. Chem.* 274, 10190–10194.
5. Andrews, N. C. (1999) *Int. J. Biochem. Cell Biol.* 31, 991–994.
6. Aisen, P., and Leibman, A. (1973) *Biochim. Biophys. Acta* 304, 797–804.
7. El Hage Chahine, J.-M., and Pakdaman, R. (1995) *Eur. J. Biochem.* 230, 1102–1110.
8. Aisen, P., Leibman, A., and Zweier, J. (1978) *J. Biol. Chem.* 253, 1930–1937.
9. Egan, T. J., Zak, O., and Aisen, P. (1993) *Biochemistry* 32, 8162–8167.
10. McFarlane, A. S. (1963) *J. Clin. Invest.* 42, 346–361.
11. Mason, A. B., Miller, M. K., Funk, W. D., Banfield, D. K., Savage, K. J., Oliver, R. W. A., Green, B. N., MacGillivray, R. T. A., and Woodworth, R. C. (1993) *Biochemistry* 32, 5472–5479.
12. Zak, O., Tam, B., MacGillivray, R. T. A., and Aisen, P. (1997) *Biochemistry* 36, 11036–11043.
13. Zak, O., and Aisen, P. (1985) *Biochim. Biophys. Acta* 829, 348–353.
14. Frieden, E., and Aisen, P. (1980) *Trends Biochem. Sci.* 5, 11.
15. Aisen, P., Aasa, R., Malmström, B. G., and Vänngård, T. (1967) *J. Biol. Chem.* 242, 2484–2490.
16. Zak, O., Aisen, P., Crawley, J. B., Joannou, C. L., Patel, K. J., Rafiq, M., and Evans, R. W. (1995) *Biochemistry* 34, 14428–14434.
17. He, Q. Y., Mason, A. B., Nguyen, V., MacGillivray, R. T. A., and Woodworth, R. C. (2000) *Biochem. J.* 350, 909–915.
18. Kretchmar, S. A., and Raymond, K. N. (1988) *Inorg. Chem.* 27, 1436–1441.
19. Zak, O., Leibman, A., and Aisen, P. (1983) *Biochim. Biophys. Acta* 742, 490–495.
20. Day, C. L., Stowell, K. M., Baker, E. N., and Tweedie, J. W. (1992) *J. Biol. Chem.* 267, 13857–13862.
21. Zak, O., Trinder, D., and Aisen, P. (1994) *J. Biol. Chem.* 269, 7110–7114.
22. Zak, O., and Aisen, P. (2002) *Biochemistry*, in press.
23. Bruns, C. M., Nowalk, A. J., Arvai, A. S., McTigue, M. A., Vaughan, K. G., Mietzner, T. A., and McRee, D. E. (1997) *Nat. Struct. Biol.* 4, 919–924.
24. Schlabach, M. R., and Bates, G. W. (1975) *J. Biol. Chem.* 250, 2182–2188.
25. Anderson, B. F., Baker, H. M., Norris, G. E., Rice, D. W., and Baker, E. N. (1989) *J. Mol. Biol.* 209, 711–734.
26. Kurokawa, H., Mikami, B., and Hirose, M. (1995) *J. Mol. Biol.* 254, 196–207.
27. MacGillivray, R. T. A., Moore, S. A., Chen, J., Anderson, B. F., Baker, H., Luo, Y. G., Bewley, M., Smith, C. A., Murphy, M. E. P., Wang, Y., Mason, A. B., Woodworth, R. C., Brayer, G. D., and Baker, E. N. (1998) *Biochemistry* 37, 7919–7928.
28. Patch, M. G., and Carrano, C. J. (1981) *Inorg. Chim. Acta* 56, L71–L73.
29. He, Q. Y., Mason, A. B., Woodworth, R. C., Tam, B. M., MacGillivray, R. T. A., Grady, J. K., and Chasteen, N. D. (1997) *Biochemistry* 36, 14853–14860.
30. Faber, H. R., Baker, C. J., Day, C. L., Tweedie, J. W., and Baker, E. N. (1996) *Biochemistry* 35, 14473–14479.
31. Aisen, P., Enns, C., and Wessling-Resnick, M. (2001) *Int. J. Biochem. Cell Biol.* 33, 940–959.
32. Trinder, D., Zak, O., and Aisen, P. (1996) *Hepatology* 23, 1512–1520.
33. Andrews, N. C., Fleming, M. D., and Gunshin, H. (1999) *Nutr. Rev.* 57, 114–123.
34. Kawabata, H., Yang, S., Hirama, T., Vuong, P. T., Kawano, S., Gombart, A. F., and Koeffler, H. P. (1999) *J. Biol. Chem.* 274, 20826–20832.
35. Anderson, B. F., Baker, H. M., Norris, G. E., Rumball, S. V., and Baker, E. N. (1990) *Nature* 344, 784–787.
36. Grossmann, J. G., Neu, M., Evans, R. W., Lindley, P. F., Appel, H., and Hasnain, S. S. (1993) *J. Mol. Biol.* 229, 585–590.
37. Tsunoo, H., and Sussman, H. H. (1983) *Arch. Biochem. Biophys.* 225, 42–54.
38. Lebrón, J. A., Bennett, M. J., Vaughn, D. E., Chirino, A. J., Snow, P. M., Mintier, G. A., Feder, J. N., and Bjorkman, P. J. (1998) *Cell* 93, 111–123.
39. Dautry-Varsat, A., Ciechanover, A., and Lodish, H. F. (1983) *Proc. Natl. Acad. Sci. U.S.A.* 80, 2258–2262.
40. Cazzola, M., Huebers, H. A., Sayers, M. H., MacPhail, A. P., Eng, M., and Finch, C. A. (1985) *Blood* 66, 935–939.
41. Young, S. P., Bomford, A., and Williams, R. (1984) *Biochem. J.* 219, 505–510.
42. Rawas, A., Muirhead, H., and Williams, J. (1997) *Acta Crystallogr., Sect. D* 53, 464–468.
43. Grossmann, J. G., Crawley, J. B., Strange, R. W., Patel, K. J., Murphy, L. M., Neu, M., Evans, R. W., and Hasnain, S. S. (1998) *J. Mol. Biol.* 279, 461–472.
44. Grossmann, J. G., Neu, M., Pantos, E., Schwab, F. J., Evans, R. W., Townes-Andrews, E., Lindley, P. F., Appel, H., Thies, W.-G., and Hasnain, S. S. (1992) *J. Mol. Biol.* 225, 811–819.
45. Mason, A. B., Tam, B. M., Woodworth, R. C., Oliver, R. W. A., Green, B. N., Lin, L. N., Brandts, J. F., Savage, K. J., Lineback, J. A., and MacGillivray, R. T. A. (1997) *Biochem. J.* 326, 77–85.
46. Evans, R. W., Crawley, J. B., Garratt, R. C., Grossmann, J. G., Neu, M., Aitken, A., Patel, K. J., Meilak, A., Wong, C., Singh, J., Bomford, A., and Hasnain, S. S. (1994) *Biochemistry* 33, 12512–12520.